

Received October 7, 2021, accepted October 18, 2021, date of publication October 27, 2021, date of current version November 8, 2021.

Digital Object Identifier 10.1109/ACCESS.2021.3123792

A Coordinated Bidding Model for Wind Plant and Compressed Air Energy Storage Systems in the Energy and Ancillary Service Markets Using a Distributionally Robust Optimization Approach

MOHSEN ALDAADI¹, (Student Member, IEEE),
FAHAD AL-ISMAIL^{1,2,3}, (Senior Member, IEEE),
ALI T. AL-AWAMI^{1,2,4}, (Senior Member, IEEE),
AND AMMAR MUQBEL¹, (Student Member, IEEE)

¹Department of Electrical Engineering, King Fahd University of Petroleum and Minerals (KFUPM), Dhahran 31261, Saudi Arabia

²K. A. CARE Energy Research and Innovation Center (ERIC), King Fahd University of Petroleum and Minerals (KFUPM), Dhahran 31261, Saudi Arabia

³Interdisciplinary Research Center for Renewable Energy and Power Systems, King Fahd University of Petroleum and Minerals (KFUPM), Dhahran 31261, Saudi Arabia

⁴Interdisciplinary Research Center for Smart Mobility and Logistics, King Fahd University of Petroleum and Minerals (KFUPM), Dhahran 31261, Saudi Arabia

Corresponding author: Fahad Al-Ismail (fsalismail@kfupm.edu.sa)

This work was supported by the Deanship of Research Oversight and Coordination (DROC) at the King Fahd University of Petroleum and Minerals (KFUPM) under Project DF201005.

ABSTRACT Clean energy resources, like wind, have a stochastic nature, which involves uncertainties in the power system. Introducing energy storage systems (ESS) to the network can compensate for the uncertainty in wind plant output and allow the plant to participate in ancillary service markets. Advance in compressed air energy storage system (CAES) technologies and their fast response make them suitable for ancillary services. This paper investigates the participation of a combined energy system composed of wind plants and compressed air energy storage system (CAES) in the energy market from a private owner's viewpoint, including trading in energy markets and bidding for frequency regulation and reserve capacity in ancillary service markets. Since this problem contains various uncertainties associated with market prices, wind generation levels, and regulation signals, distributionally robust optimization (DRO) is used to model the uncertainties and enhance the simultaneous participation of a combined wind-CAES system in day-ahead energy and ancillary service markets. This method combines the advantages of stochastic and robust optimization. In contrast to robust optimization (RO), the method consolidates specific statistical data to reduce conservative results. Simulation results demonstrate the proposed model's effectiveness in handling uncertainties and provide a framework for investors in this area. In addition, case study analyses are applied to assess the model's performance and validate the coordination of a wind plant and compressed air energy storage system in participating in a deregulated electricity market. Finally, DRO and RO are compared in modeling the uncertainties of the optimization problem. The optimal outputs demonstrate the effectiveness of DRO in terms of achieving higher realized profits with less conservative results.

INDEX TERMS Wind power operation, compressed air energy storage, energy market, distributionally robust optimization, linear decision rule.

I. NOMENCLATURE

SETS AND INDICES

t Index of time.
 T Set of Time.

The associate editor coordinating the review of this manuscript and approving it for publication was Mouloud Denai¹.

SUPERSCRIPTS

ch CAES charge power superscript.
 d CAES discharge power superscript.
 DA Day-ahead bids superscript.
 e Energy market superscript.
 g Generated power of wind plant superscript.
 reg Regulation market superscript.
 rt Real time market.

m	Regulation movement.
Ng	Natural gas superscript.
sr	Spinning reserve superscript.
sc	CAES simple cycle operation mode superscript.
w	Wind farm bid superscript.
\sim	Superscript for uncertain parameter.

PARAMETERS

E_{min}	Minimum energy capacity, MWh .
E_{max}	Maximum energy capacity, MWh .
E_i^{st}	Energy amount of CAES in the beginning of the day, MWh .
E^{INT}	Energy amount of CAES in the end of the day, MWh .
P_{max}^{Com}	Maximum charging power rate of CAES, MWh .
P_{max}^{Exp}	Maximum discharging power rate of CAES, MWh .
OC	Operating cost.
HR	Heat rate of CAES, GJ/MWh .
R_{mil}	Total of absolute vaules of AGC movements, $\Delta MW/MW$.
P	Power capacity, MWh .
VOM	Variable operation and maintenance cost of CAES, $\$/MWh$.
α_{call}	Status of spinning reserve capacity call.
β_t	Average energy used in regulation up or down during hour t , MWh .
γ_t	Market prices, $\$/MWh$.
η	Efficiency of CAES.
Π^{Ng}	Price of Natural gas.

DECISION VARIABLES

P_t^{DA}	Total day-ahead bid capacity at time t , MWh
P_t^c	CAES day-ahead bid capacity at time t , MWh
P_t^w	Wind plant bid capacity at time t , MWh .
P_t^d	CAES discharge capacity at time t , MWh .
P_t^{sc}	CAES simple cycle operation mode capacity at time t , MWh .
P_t^{ch}	CAES charge capacity at time t , MWh .
$P_t^{sc, sr}$	CAES spinning reserve participating capacity in simple cycle mode at time t , MWh .
$P_t^{d, sr}$	CAES spinning reserve participating capacity in discharging mode at time t , MWh .
$P_t^{d, reg}$	CAES regulation participating capacity in discharging mode at time t , MWh .
$P_t^{sc, reg}$	CAES regulation participating capacity in simple cycle mode at time t , MWh .
E_t	CAES state of charge, MWh .
$\alpha_t^{ch, d, sc}$	Binary variables for either charging, discharging or operating in simple cycle mode at time t .

OTHERS

$\mathbb{E}_{\mathbb{P}}$	Expected value under distribution \mathbb{P} .
$g_n(\cdot)$	Quadratic representable functions characterizing the distributions of random variables \mathbf{c} .

$\mathcal{L}(\cdot)$	Function indicating energy not served.
\mathbb{P}	A distribution of all random variables \mathbf{c} .
\mathbb{Q}	A distribution of all random variables \mathbf{c} and auxiliary variables $\boldsymbol{\omega}$.
$\mathcal{Q}_0(\cdot)$	Set of all distributions for random variables with the given dimension.
$ \cdot $	The cardinality of a set or the absolute value of a mathematical expression.
$\ \cdot\ $	The 2-norm of a vector.

II. INTRODUCTION

A. BACKGROUND AND PROBLEM DESCRIPTION

Wind uncertainty poses a significant challenge for wind farm owners participating in a deregulated market. Under standard market design (SMD), energy offers from generation owners and price bids from retailers are submitted on a day-ahead basis to the independent system operator (ISO), who decides the dispatch schedule by solving an optimization problem. Since wind energy is a non-dispatchable resource, scheduling offers, even with an accurate forecast, is a challenge [1]. With the need for large-scale penetration of renewable resources, energy storage systems (ESS) would be a preferable technology to improve wind plant performance when synchronized with the bulk power system. This improvement is due to the ability of ESS to absorb and deliver power to the grid quickly, an ability which could be exploited to mitigate the uncertainty of wind power.

There are different large-scale ESSs that could dispatch wind energy to maximize the benefits of the arbitrage market, such as pumped storage, chemical batteries, and compressed air energy storage systems (CAES). Compared to pumped storage and chemical batteries, CAES has lower investment costs and fewer construction limits [2], [3]. Furthermore, CAESs have longer life expectancies and higher charge and discharge efficiencies [4]. Moreover, CAES can work as a regular gas turbine, which is called simple cycle operation mode. Simple cycle mode makes CAES different than the other types of storage systems, which allows the CAES to better follow an everyday operation schedule [5]. Currently, the focus of related research is on fabricating and designing a storage reservoir for a CAES to store air of a higher pressure and to eliminate dependency on geological sites [6].

B. LITERATURE REVIEW

In the literature, several studies have focused on estimating the economic value of either CAES alone or coupled with wind plants when participating in a deregulated market [7]–[10]. An economic analysis was conducted in [7] to evaluate CAES revenues in French regulated and deregulated electricity markets. With an optimum CAES capacity calculated for a wind plant, the daily profit from the energy market for a whole year was evaluated based on particle swarm optimization (PSO). Further, a sensitivity analysis was included in [8]. An optimal dispatch algorithm using dynamic

programming to maximize CAES's expected profit coupled with a wind plant in the energy market was constructed in [9]. In [10], an optimal operating model for a CAES system participating in the ancillary service market, namely regulation and reserve, is proposed to maximize profits. The whole model was formulated using mixed-integer linear programming (MILP) and solved using real-time market data. In the research mentioned above, uncertainty associated with different parameters in the optimization problem, such as prices, wind power output, and deployment of ancillary services, have been ignored. These uncertainties could significantly affect revenue since forecasting error can fluctuate remarkably depending on market mechanisms and other factors associated with the prediction method [11]. As a result, uncertainty should be addressed when modeling bidding strategies and scheduling operations for wind power generation coupled with a CAES system.

In [12], a WP and CAES system was proposed to participate in the energy market by bidding capacity. Uncertainties in market prices were handled using adaptive robust optimization. Stochastic optimization was used in [5] to handle the aggregation of WP and CAES. Risk-constrained bidding was used to participate in the day-ahead market. In [12] and [5], the simple cycle mode of a CAES was considered, where the CAES can work as a gas turbine when needed. However, the papers focused on bidding in the energy market and did not consider bidding reserve and regulation capacities in the ancillary services market. In [13], the operation of the WP and CAES system was optimized to maximize profits from bidding in the day-ahead energy market and spinning reserve. Although the stochastic approach was used to handle uncertainties, the simple cycle mode of the CAES and regulation participation were not considered in this paper. In [14], the CAES model is proposed to reduce the operation cost of the system considering the support of reactive power. In reference [15], an advanced adiabatic compressed air energy storage (AA-CAES) with tri-state system is proposed and integrated with the dispatch problem to minimize the cost of energy. In [14] and [15], the simple cycle mode of the CAES is not considered. In addition, the market environment, where the system of CAES and wind plant are bidding for capacity in the energy and ancillary services market and receiving the regulation signals in real-time, is not considered. In addition, the different uncertainties associated with the system are not considered. Wind-thermal-photo-voltaic and wind-thermal-energy storage systems were proposed to participate in the energy market in [16] and energy spinning reserve markets in [17]. Multi-objective optimization was proposed to maximize profit while minimizing emissions from thermal units. Scenarios were generated and used to represent uncertainties in market prices and renewable outputs.

Several methods have been used to deal with uncertainty in optimization problems. In [18], stochastic programming was used to address uncertain parameters in bidding strategies. This approach tried to optimize expected profit considering the exact distribution of uncertainties. This method requires

the exact probability distribution of uncertain parameters and a huge number of scenarios. As the number of scenarios grows, the size of the optimization function increases drastically. Fuzzy optimization is another method that has been used to handle uncertainties as proposed in [19] to model uncertainties in a virtual power plant (VPP). This method requires a good estimation of error in the available data and a good definition of the system operator's uncertainty limits. Robust Optimization (RO) has also been used in [20] and [21] to address uncertainty in the optimization problems. This approach is a deterministic approach based on the structure of an optimization that guarantees the feasibility of realizing an unpredictable parameter over a support set. However, in this approach, it is challenging to incorporate distribution information accurately. Further, the worst-case realization is sometimes too pessimistic in modeling system uncertainties, resulting in over-conservative solutions [3]. Two stage chance constraint stochastic programming, a relatively robust approach, is used in [22] for the energy hub operators to participate in the day-ahead and real-time energy market. This approach guarantees the probability of meeting a specific constraint is above a certain level.

A new approach, Distributionally Robust Optimization (DRO), overcomes the limitations of the methods mentioned above. This kind of optimization addresses the uncertainty associated with some parameters by utilization of an ambiguity set which incorporates partial distribution information such as support sets, mean values, and variances [23]. DRO can optimize the expected value by effectively leveraging statistical information and avoiding the presumption of knowing the exact probability distribution of a random variable as is the case in SP. Besides, this partial statistical information can improve DRO's performance and yield more optimistic results compared to the conservatism associated with RO problems. Due to the merit of this approach, DRO has been used recently in different power system problems, e.g., energy and reserve scheduling [24], [25], solving for unit commitment [26], and determining the optimal allocation of wind farms in a multi-area power system [27]. However, DRO has not been used in handling the uncertainties of a wind plant and CAES system when participating in the energy and ancillary services market.

C. CONTRIBUTION

In this paper, a comprehensive framework is proposed for coordinated bidding of a wind plant and CAES system in order to maximize profit from participation in energy and ancillary service markets. The main contributions of this paper are:

- 1) The model is formulated as linear equations to promote the profitability of a coordinated wind plant and CAES system with incorporating simple cycle mode, where the CAES works as gas turbine, and manage the bidding of the system in the day-ahead energy and ancillary services market.

$$E_{t+1} = E_t + P_t^{ch} \eta_c - \frac{(P_t^d + \alpha_t^{sr} P_t^{sr,d})}{\eta_d}$$

$$OC = (P_t^d + P_t^{d,sr} \cdot \alpha_{call}^{sr} + 2 \cdot \beta_t \cdot P_t^{d,reg}) \cdot (HR^d \cdot \Pi^{Ng} + VOM^d) + (P_t^{sc} + P_t^{sc,sr} \cdot \alpha_{call}^{sr} + 2 \cdot \beta_t \cdot P_t^{sc,reg}) \cdot (HR^{sc} \cdot \Pi^{Ng} + VOM^{sc}) + P_t^{ch} \cdot VOM^{ch} \quad (15)$$

$$(16)$$

The first part of the objective function (1) includes energy arbitrage revenue of the wind farm and CAES from the day-ahead energy market. The second is the CAES’s capacity revenue from participating in spinning reserve when working in discharge mode or simple cycle mode. The third part is the payment for providing capacity to the regulation market. As aforementioned in the market structure, the fourth part is an extra payment based on real-time prices for the called capacity in the reserve market. The pay-for-performance structure is modeled in the fifth part. The last part is the operation cost, expressed as operation cost during discharge mode, simple cycle mode, and charge mode. The operation cost is shown in constraint (16) as a function of the natural gas price and the variable operation and maintenance costs of the CAES in discharging and simple cycle modes, and as a function of only the variable operation and maintenance costs in charging mode.

Since the CAES system can only operate in charge, simple cycle, or discharge mode at a specified time, constraint (2) limits overlapping operations where α_t^{ch} , α_t^d and α_t^{sc} are binary variables. Constraint (3) implies the hourly day-ahead bids as a function of wind plant bids and CAES bids. As shown in constraint (4), CAES bids integrate the three operation modes. Constraints (5) and (6) limit wind plant and CAES bids to their maximum and minimum capacities. Constraint (7) restricts the CAES’s charging power to its maximum and minimum limits. Similarly, (8), (9), and (10) constrain injected power from the CAES, in discharge or simple cycle mode, to its power capacity limits. Bidding in the regulation market should be less than or equal to the energy market bid (11). In addition, the CAES needs to have some energy to prepare itself for the next day (12). The energy constraints of the CAES are stated in (13) and (14). Constraint (15) describes the dynamic behavior of the CAES.

IV. PROBLEM REFORMULATION USING DISTRIBUTIONALLY ROBUST OPTIMIZATION

A. UNCERTAINTY AND COMPACT MATRIX FORMULATION

Generally, in the day-ahead electricity and ancillary service markets, participants are required to submit their bids several hours before the start of the operating day. For instance, NYISO requires participants to bid and offer for the following day at 5 AM of the current day [29]. The gap between the bidding time and the operation day can be from 19 to 43 hours, resulting in a highly uncertain wind forecast. Furthermore, bidding will depend on other uncertain forecasts such as market prices, spinning reserve, and AGC signals. As a result, a two-stage distributionally robust optimization is proposed to schedule bid decisions in the first stage. Then,

in the second stage, decisions related to the CAES and wind plant operation are made after the uncertainties have been uncovered. Hence, the extracted solution of the two-stage DRO optimization is a single one-stage policy with corrective actions made in response to system uncertainties [30].

The uncertain parameters and the decision variables are defined to express the problem (1) compactly. The presentation of the compact matrix formulation is to simplify the analysis of the reformulation using DRO. Throughout the reformulation, matrices and vectors are expressed by bold lowercase letters, while entries of matrices and vectors are represented by regular letters with subscripts denoting the indices. The decision variables in the objective function (1) are $\{P_t^w, P_t^d, P_t^{sc}, P_t^{ch}, P_t^{d,sr}, P_t^{sc,sr}, P_t^{d,reg}, P_t^{sc,reg}, \alpha_t^{ch}, \alpha_t^d, \alpha_t^{sc}\}$ while the uncertain parameters are $\{P^g, \gamma^e, \gamma^{sr}, \gamma^{reg}, \gamma^{reg,m}, \gamma^{rt}, \alpha_{call}^{sr}, R_{mil}\}$. In the first stage, decision variables $\{\alpha_t^{ch}, \alpha_t^d, \alpha_t^{sc}\}$ are determined before the realization of future uncertainty which is represented by $\mathbf{x} \in \mathbb{R}^{|\mathcal{K}|}$, where \mathcal{K} is the set of all decision variables. The second stage’s decision variables $\{P_t^w, P_t^d, P_t^{sc}, P_t^{ch}, P_t^{d,sr}, P_t^{sc,sr}, P_t^{d,reg}, P_t^{sc,reg}\}$ are expressed by a vector \mathbf{y} , which are determined over an ambiguity set \mathbb{G} . Hence the objective (1) and constraints (2)-(16) are of the form:

$$\min \sup_{\mathbb{P} \in \mathbb{G}} \mathbb{E}_{\mathbb{P}} \{ \mathcal{L}(\mathbf{x}, \tilde{\mathbf{c}}) \} \quad (17)$$

$$\text{s.t. } \mathbf{A}\mathbf{x} \leq \mathbf{b} \quad (18)$$

$$\mathbf{x}_i \in \{0, 1\} \quad \forall i \in \mathbb{B} \subseteq \{1, n\} \quad (19)$$

with $\mathbf{A} \in \mathbb{R}^{|\mathcal{V}| \times |\mathcal{K}|}$ and $\mathbf{b} \in \mathbb{R}^{|\mathcal{V}|}$; where \mathcal{V} is the set of all constraints. The function $\mathcal{L}(\mathbf{x}, \mathbf{c})$ is determined in the second-stage with the effect of uncertain parameters, and this function is expressed by

$$\mathcal{L}(\mathbf{x}, \mathbf{c}) = \min \mathbf{f}^T \mathbf{y} \quad (20)$$

$$\text{s.t. } \mathbf{E}(\mathbf{c}) + \mathbf{T}\mathbf{y} \leq \mathbf{q}(\mathbf{c}) \quad (21)$$

In this expression, $\mathbf{f} \in \mathbb{R}^{|\mathcal{K}|}$, $\mathbf{E}(\mathbf{c}) \in \mathbb{R}^{|\mathcal{V}| \times |\mathcal{K}|}$, $\mathbf{T} \in \mathbb{R}^{|\mathcal{V}| \times |\mathcal{K}|}$, and $\mathbf{q}(\mathbf{c}) \in \mathbb{R}^{|\mathcal{V}|}$. Constraints of the second stage problem are included as an inequality constraint which is suggested by (21) where the right-hand-side matrix $\mathbf{E}(\mathbf{c})$ and the left-hand-side vector $\mathbf{q}(\mathbf{c})$ are influenced by the uncertain parameter \mathbf{c} . The matrix $\mathbf{E}(\mathbf{c})$ and vector $\mathbf{q}(\mathbf{c})$ are expressed as the following linear affine equations:

$$\mathbf{E}(\mathbf{c}) = \mathbf{E}^0 + \sum_{m \in \mathcal{M}} \mathbf{E}_m^c c_m \quad (22)$$

$$\mathbf{q}(\mathbf{c}) = \mathbf{q}^0 + \sum_{m \in \mathcal{M}} \mathbf{q}_m^c c_m \quad (23)$$

B. AMBIGUITY SETS

The uncertain parameters of the objective function (1) are modeled using an ambiguity set \mathbb{G} that defines a family of distributions [31]. Wind uncertainty can be modeled in the ambiguity set using the expressions (24)-(27).

$$\mathbb{P} \{ \tilde{\mathbf{P}}^g \in \mathcal{W} \} = 1 \quad (24)$$

$$\mathbb{E}_{\mathbb{P}} \left\{ \tilde{P}_t^g \right\} = \bar{P}_t^g, \quad \forall t \in \mathcal{T} \quad (25)$$

$$\mathbb{E}_{\mathbb{P}} \left\{ |\tilde{P}_t^g - \bar{P}_t^g| \right\} \leq \phi_t^w, \quad \forall t \in \mathcal{T}, \quad (26)$$

$$\mathbb{E}_{\mathbb{P}} \left\{ (\tilde{P}_t^g - \bar{P}_t^g)^2 \right\} \leq \lambda_t^w, \quad \forall t \in \mathcal{T} \quad (27)$$

The first constraint (24) guarantees that the uncertainty associated with wind power generation is bounded using a support set \mathcal{W} . Similar to conventional robust optimization, the support set \mathcal{V} is fixed to its lower and upper bound by (28):

$$\mathcal{W} = \left\{ P_t^g \mid P_t^{g-} \leq P_t^g \leq P_t^{g+}, \forall t \in \mathcal{T} \right\} \quad (28)$$

The second constraint (25) indicates that the generalized moment of $\mathbb{E}_{\mathbb{P}} \left\{ \tilde{P}_t^g \right\}$ is \bar{P}_t^g . The inequality constraint (26) implies that the mean absolute deviation of \tilde{P}_t^g is not higher than ϕ_t^w . Lastly, the variance in (27) is less than or equal to the constant λ_t^w . Obviously, equations (24)-(27) characterize statistical measures such as expectation, mean absolute deviation, and variance, which could be estimated using historical data without the need for an exact probability distribution as is the case in stochastic programming.

The statistical distribution measures of market prices are modeled in the ambiguity set using the constraints (29)-(32). Note that these constraints are generalized for all uncertain market prices in the problem.

$$\mathbb{P} \left\{ \tilde{\gamma} \in \mathcal{P} \right\} = 1 \quad (29)$$

$$\mathbb{E}_{\mathbb{P}} \left\{ \tilde{\gamma}_t \right\} = \bar{\gamma}_t, \quad \forall t \in \mathcal{T} \quad (30)$$

$$\mathbb{E}_{\mathbb{P}} \left\{ |\tilde{\gamma}_t - \bar{\gamma}_t| \right\} \leq \phi_t^p, \quad \forall t \in \mathcal{T}, \quad (31)$$

$$\mathbb{E}_{\mathbb{P}} \left\{ (\tilde{\gamma}_t - \bar{\gamma}_t)^2 \right\} \leq \lambda_t^p, \quad \forall t \in \mathcal{T} \quad (32)$$

The first constraint (29) ensures that random market prices are bounded using a support set, \mathcal{P} . The support set \mathcal{P} is defined with its lower and upper bounds by equation (33).

$$\mathcal{P} = \left\{ \gamma \mid \gamma_t^- \leq \gamma_t \leq \gamma_t^+, \forall t \in \mathcal{T} \right\} \quad (33)$$

The constraints (30)-(32) represent the expectation, the mean absolute deviation, and the variance, which could be determined from historical market price data.

Considering the unpredictable behavior of reserve deployment and regulation signals, we adopted a similar procedure [28] to handle them. For reserve deployment uncertainty, the worst-case scenario of the historical data is introduced, where the uncertainty of regulation signals are ignored due to their negligible effect. A compact matrix that provides for all the mentioned constraints is expressed as follows:

$$\mathbb{G} = \left\{ \mathbb{P} \in \mathcal{Q}_0 \left(\mathbb{R}^{|\mathcal{M}|} \right) : \begin{array}{l} \tilde{\mathbf{c}} \in \mathbb{R}^{|\mathcal{M}|} \\ \mathbb{P} \left\{ \tilde{\mathbf{c}} \in \mathcal{C} \right\} = 1 \\ \mathbb{E}_{\mathbb{P}} \left\{ \tilde{c}_m \right\} = \bar{c}_m, \quad \forall m \in \mathcal{M} \\ \mathbb{E}_{\mathbb{P}} \left\{ g_n(\tilde{\mathbf{c}}) \right\} \leq \mu_n, \quad \forall n \in \mathcal{N} \end{array} \right\} \quad (34)$$

The uncertain parameters (24) and (29) are combined in the vector $\tilde{\mathbf{c}}$, where \mathcal{M} is the set of distributions in $\mathbb{R}^{|\mathcal{M}|}$. The following constraint in (34) implies that all distributions of the random vector $\tilde{\mathbf{c}}$ are within a support set \mathcal{C} , which includes all the support sets (28) and (33). The third constraint

in (34) is the expected value of random variables, which is a generalized form of the constraints (25) and (30). The last constraint in (34) characterizes distribution information of uncertainties via $g_n(\tilde{\mathbf{c}})$, which is a compact form of the absolute deviation and variance. The expected value of $g_n(\tilde{\mathbf{c}})$ expresses the all inequality constraints (26), (31), (27), (32), where the constants $\phi_t^w, \lambda_t^w, \phi_t^p,$ and λ_t^p are represented by μ_n .

Due to the difficulty of estimating the expectation of each function $g_n(\tilde{\mathbf{c}})$ under uncertain distributions, the proposed problem is too complicated to be solved. To derive a tractable formulation, a set of auxiliary variables is included in the ambiguity set to address the functions' upper bound.

A new joint family of distributions denoted by \mathbb{Q} is introduced for both the random and auxiliary variables. The support set is extended to (35).

$$\tilde{\mathcal{C}} = \left\{ (\mathbf{c}, \boldsymbol{\omega}) \in \mathbb{R}^{|\mathcal{M}|} \times \mathbb{R}^{|\mathcal{N}|} : \begin{array}{l} \mathbf{c} \in \mathcal{C} \\ g_n(\mathbf{c}) \leq \omega_n, \quad \forall n \in \mathcal{N} \\ \omega_n \leq \sup_{\mathbf{c} \in \mathcal{C}} g_n(\mathbf{c}), \quad \forall n \in \mathcal{N} \end{array} \right\} \quad (35)$$

The extended support set implies that the function $g_n(\mathbf{c})$ is bounded from the top by ω_n . Hence, the expected value in (35) cannot hold unless the fourth line in (34) is satisfied. Since the support set \mathcal{C} is composed of linear expressions(24) and (29) and the function $g_n(\mathbf{c})$ is either quadratic or linear defining various moment information, these functions are converted into the following second-order cone constraints [27]. Accordingly, a dual formulation can be derived simply in the next subsection.

$$\tilde{\mathcal{C}} = \left\{ (\mathbf{c}, \boldsymbol{\omega}) \in \mathbb{R}^{|\mathcal{M}|} \times \mathbb{R}^{|\mathcal{N}|} : \begin{array}{l} \|\mathbf{F}_r \mathbf{c} + \mathbf{H}_r \boldsymbol{\omega} - \mathbf{h}_r\| \\ \leq \mathbf{a}_r^T \mathbf{c} + \mathbf{s}_r^T \boldsymbol{\omega} + e_r, \quad r \in \mathcal{R} \end{array} \right\} \quad (36)$$

with $\mathbf{F}_r \in \mathbb{R}^{V_r \times |\mathcal{M}|}, \mathbf{H}_r \in \mathbb{R}^{V_r \times |\mathcal{N}|},$ and $\mathbf{h}_r \in \mathbb{R}^{V_r},$ where V_r is the row number for the r th constraint, and the set of all constraints representing the extended support set $\tilde{\mathcal{C}}$ are indicated by \mathcal{R} . The modified support set $\tilde{\mathcal{C}}$ and ambiguity set $\tilde{\mathbb{G}}$ are used to reformulate a tractable expectation problem in the next subsection.

C. REFORMULATION BASED ON GENERALIZED LINEAR DECISION RULE APPROXIMATION

In a two-stage DRO optimization problem, extracting an explicit expression of the exact optimal solution is generally intractable, since the worst-case expectation of $\mathcal{L}(\mathbf{x}, \tilde{\mathbf{c}})$ must be determined by solving the recourse policy in (20)-(21) under realization of all uncertainties within the support set $\tilde{\mathbb{G}}$ [32]. This issue is addressed by using affine decision rules (ADR), which in turn will make the recourse decision \mathbf{y} to be affinely modified with the uncertainties [33]–[36]. In this work, the decision rule function \bar{y}_k is affected by uncertain parameters \mathbf{c} and auxiliary variables $\boldsymbol{\omega}$, which are formulated as:

$$\bar{y}_k(\mathbf{c}, \boldsymbol{\omega}) = y_k^0 + \sum_{m \in \mathcal{M}_k} y_{km}^c c_m + \sum_{n \in \mathcal{N}_k} y_{kn}^\omega \omega_n, \quad \forall k \in \mathcal{K}_2 \quad (37)$$

The subset \mathcal{M}_k and \mathcal{N}_k consist of random and auxiliary variables that modify the decision \bar{y}_k for each hour. Therefore, for the day ahead, 24-hours, 24 subsets are included in this work. A further generalization of the affine decision rule \bar{y}_k is expressed as:

$$\bar{y} = \mathbf{y}^0 + \mathbf{Y}^c \mathbf{c} + \mathbf{Y}^\omega \boldsymbol{\omega} \quad (38)$$

where $\mathbf{y}^0 \in \mathbb{R}^{|\mathcal{K}|}$ denotes constant terms, and $\mathbf{Y}^c, \mathbf{Y}^\omega$ are coefficient matrices, and their entries are defined by (39) and (40), the affine coefficient terms that are respectively associated with \mathbf{c} and $\boldsymbol{\omega}$.

$$Y_{km}^c = \begin{cases} y_{km}^c, & \text{if } m \in \mathcal{M}_k \\ 0, & \text{if } m \in \mathcal{M} \setminus \mathcal{M}_k \end{cases} \quad \forall k \in \mathcal{K}_2 \quad (39)$$

$$Y_{kn}^\omega = \begin{cases} y_{kn}^\omega, & \text{if } n \in \mathcal{N}_k \\ 0, & \text{if } n \in \mathcal{N} \setminus \mathcal{N}_k \end{cases} \quad \forall k \in \mathcal{K}_2 \quad (40)$$

By substituting an affine decision rule approximation for the actual recourse decision \mathbf{y} of each uncertain realization, an approximated formulation of the two-stage DRO problem can be derived as follows:

$$\min \sup_{\mathbb{Q} \in \bar{\mathcal{G}}} \mathbb{E}_{\mathbb{Q}} \left\{ \mathbf{f}^T \mathbf{y}(\bar{\mathbf{c}}, \tilde{\boldsymbol{\omega}}) \right\} \quad (41)$$

$$\text{s.t. } \mathbf{A}\mathbf{x} \leq \mathbf{b} \quad (42)$$

$$\mathbf{E}(\mathbf{c}) + \mathbf{T}\bar{\mathbf{y}}(\mathbf{c}, \boldsymbol{\omega}) \leq \mathbf{q}(\mathbf{c}), \quad \forall (\mathbf{c}, \boldsymbol{\omega}) \in \bar{\mathcal{C}} \quad (43)$$

The above conservative formulation yields a lower bound than the expected profit gained from the wind-CAES combination. A semi-infinite representation can be written for the inner supreme as follows:

$$\sup \int_{\bar{\mathcal{C}}} \mathbf{f}^T \bar{\mathbf{y}}(\mathbf{c}, \boldsymbol{\omega}) d\mathbf{f}(\mathbf{c}, \boldsymbol{\omega}) \quad (44)$$

$$\text{s.t. } \int_{\bar{\mathcal{C}}} c_m d\mathbf{f}(\mathbf{c}, \boldsymbol{\omega}) = \bar{c}_m, \quad \forall m \in \mathcal{M} \quad (45)$$

$$\int_{\bar{\mathcal{C}}} \omega_n d\mathbf{f}(\mathbf{c}, \boldsymbol{\omega}) \leq \mu_n, \quad \forall n \in \mathcal{N} \quad (46)$$

$$\int_{\bar{\mathcal{C}}} f(\mathbf{c}, \boldsymbol{\omega}) = 1 \quad (47)$$

$$f(\mathbf{c}, \boldsymbol{\omega}) \geq 0, \quad \forall (\mathbf{c}, \boldsymbol{\omega}) \in \bar{\mathcal{C}} \quad (48)$$

The equations (41)-(43) are reformulated into the robust optimization problem below, which is derived by dualizing the semi-infinite representation (44)-(48).

$$\min \rho + \bar{\mathbf{c}}^T \boldsymbol{\eta} + \boldsymbol{\mu}^T \boldsymbol{\beta} \quad (49)$$

$$\text{s.t. } \mathbf{A}\mathbf{x} \leq \mathbf{b} \quad (50)$$

$$\rho + \mathbf{c}^T \boldsymbol{\eta} + \boldsymbol{\omega}^T \boldsymbol{\beta} \geq \mathbf{f}^T \bar{\mathbf{y}}(\mathbf{c}, \boldsymbol{\omega}), \quad \forall (\mathbf{c}, \boldsymbol{\omega}) \in \bar{\mathcal{C}} \quad (51)$$

$$\mathbf{E}(\mathbf{c})\mathbf{x} + \mathbf{T}\bar{\mathbf{y}}(\mathbf{c}, \boldsymbol{\omega}) \leq \mathbf{q}(\mathbf{c}), \quad \forall (\mathbf{c}, \boldsymbol{\omega}) \in \bar{\mathcal{C}} \quad (52)$$

$$\rho \in \mathbb{R}, \boldsymbol{\eta} \in \mathbb{R}^{|\mathcal{M}|}, \boldsymbol{\beta} \in \mathbb{R}_-^{|\mathcal{N}|} \quad (53)$$

Constraints (45), (46), and (47) are expressed by the dual variables $\boldsymbol{\eta}, \boldsymbol{\beta}$, and ρ , respectively, reaching a classic robust optimization problem with a tractable polyhedral uncertainty

set $\bar{\mathcal{C}}$, which can be represented as the following robust counterpart:

$$\min \rho + \bar{\mathbf{c}}^T \boldsymbol{\eta} + \boldsymbol{\mu}^T \boldsymbol{\beta} \quad (54)$$

$$\text{s.t. } \mathbf{A}\mathbf{x} \leq \mathbf{b} \quad (55)$$

$$\rho - \mathbf{f}^T \mathbf{y}^0 + \sum_{r \in \mathcal{R}} \left(\mathbf{h}_r^T \boldsymbol{\pi}_r^0 + e_r \zeta_r^0 \right) \geq 0 \quad (56)$$

$$\sum_{r \in \mathcal{R}} \left(\mathbf{F}_r^T \boldsymbol{\pi}_r^0 - \zeta_r^0 \mathbf{a}_r \right) = \boldsymbol{\eta} - \mathbf{Y}^c \mathbf{f} \quad (57)$$

$$\sum_{r \in \mathcal{R}} \left(\mathbf{H}_r^T \boldsymbol{\pi}_r^0 - \zeta_r^0 \mathbf{s}_r \right) = \boldsymbol{\beta} - \mathbf{Y}^\omega \mathbf{f} \quad (58)$$

$$\|\boldsymbol{\pi}_r^0\| \leq \zeta_r^0, \quad \forall r \in \mathcal{R} \quad (59)$$

$$\boldsymbol{\pi}_r^0 \in \mathbb{R}^{V_r}, \zeta_r^0 \in \mathbb{R}_+, \quad \forall r \in \mathcal{R} \quad (60)$$

$$\left(\mathbf{E}^0 \mathbf{x} + \mathbf{y}^0 \right)_v \leq q_v^0 + \sum_{r \in \mathcal{R}} \left(\mathbf{h}_r^T \boldsymbol{\pi}_r^v + e_r \zeta_r^v \right), \quad (61)$$

$$\forall v \in \mathcal{V}_2 \quad (61)$$

$$\sum_{r \in \mathcal{R}} \left(\mathbf{F}_r^T \boldsymbol{\pi}_r^v - \zeta_r^v \mathbf{a}_r \right)_m = (\mathbf{d}^m - \mathbf{E}^m \mathbf{x})_v - (\mathbf{T}\mathbf{Y}^c)_{vm}, \quad (62)$$

$$\forall m \in \mathcal{M}, \forall v \in \mathcal{V}_2 \quad (62)$$

$$\sum_{r \in \mathcal{R}} \left(\mathbf{H}_r^T \boldsymbol{\pi}_r^v - \zeta_r^v \mathbf{s}_r \right)_m = -(\mathbf{T}\mathbf{Y}^c)_{vm}, \quad (63)$$

$$\forall m \in \mathcal{M}, \forall v \in \mathcal{V}_2 \quad (63)$$

$$\|\boldsymbol{\pi}_r^0\| \leq \mu_r^0, \quad \forall r \in \mathcal{R} \quad (64)$$

$$\boldsymbol{\pi}_r^v \in \mathbb{R}^{V_r}, \mu_r^v \in \mathbb{R}_+, \quad \forall r \in \mathcal{R}, \forall v \in \mathcal{V}_2 \quad (65)$$

$$\rho \in \mathbb{R}, \boldsymbol{\eta} \in \mathbb{R}^{|\mathcal{M}|}, \boldsymbol{\beta} \in \mathbb{R}_-^{|\mathcal{N}|} \quad (66)$$

The constraints (56)-(60) are the reformulation of the constraint (51) after dualizing the extended ambiguity set $\bar{\mathcal{C}}$. The vectors $\boldsymbol{\pi}_r^0$ and μ_r^0 are denoted for dual variables. In the same manner, by considering dual variables $\boldsymbol{\pi}_r^m$ and μ_r^m , constraints (61)-(65) are derived from the m th constraint (52). The robust counterpart of the formulated two-stage operation problem is a convex second-order cone programming problem. After applying the affine decision rule, linear optimization programming might be conservative, resulting in a much lower computational burden than the original two-stage optimization problem. Based on a case study, the effectiveness of the proposed model is demonstrated in the next section.

V. CASE STUDIES

A. CASE STUDY DESCRIPTION

A producer was assumed to own and operate a 32MW wind plant and a 15 MWh CAES. The optimal bidding strategy was determined based on a two-stage DRO approach. Historical market and operational data were taken from the NYISO website [37]. Historical wind power data for a hypothetical wind power plant located in New York was used, available on the NREL website [38]. The constants of the ambiguity sets were calculated using historical data for each hour of the operating day and were included to solve the DRO problem. The characteristics of the CAES were obtained from [5]. The two-stage DRO problem was solved using an IBM ILOG

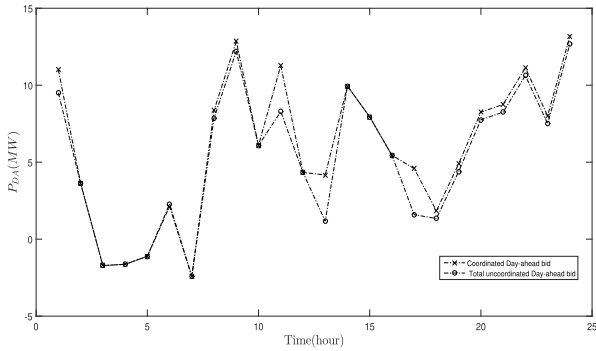


FIGURE 2. Day-ahead dispatch in the energy and ancillary services markets.

CPLEX solver in the MATLAB programming language, and the PC used had an Intel Core 7 CPU (2.5 GHz) and 8.0 GB RAM.

B. COORDINATED AND UNCOORDINATED BIDDING OF A WIND PLANT AND CAES SYSTEM USING DRO

The optimal bidding strategy for coordinated and uncoordinated participation of the wind plant and CAES in energy and ancillary service markets using DRO can be determined as shown in Figs. 2 and 3. Bids were obtained for both cases based on the worst-case expected total wind generation P_g and other uncertain prices. For the demonstration, the CAES bids were added to the wind plant bids for the uncoordinated case and the results were compared to the coordinated bids, as shown in Fig. 2. It is clear that in the coordinated case more power is dispatched over a number of hours, starting from hour 8 to the end of the day. This was because, due to the flexibility of coordinated bids, the CAES was able to store wind energy until it was able to take advantage of a period when prices were higher. The CAES operation demonstrated in the first graph of Fig. 3 illustrates the CAES bids in the coordinated case. The CAES was charged by wind plant from hours 2 to 5 since prices were low and extra charging capacity was taken from the energy market. In contrast, the second graph of Fig. 3 shows that in the uncoordinated case, the CAES was charged by the market, and the wind plant was forced to sell its power when prices were low.

In Table (1), realized profits for coordinated and uncoordinated bidding of the wind plant and the CAES were calculated based on real data. As shown in Table (1), the expected worst-case profits and the realized profits were determined for both cases. The expected worst-case and the realized profit were higher for the coordinated bids than the uncoordinated bids, which demonstrates the CAES’s effectiveness in enhancing profits when integrated with a wind plant.

C. COMPARISON OF USING DRO AND ROBUST OPTIMIZATION FOR COORDINATED BIDDING OF A WIND PLANT AND CAES SYSTEM

Two cases are introduced in this section to fully illustrate how much better the performance of coordinated bidding using DRO is than the performance of coordinated bidding

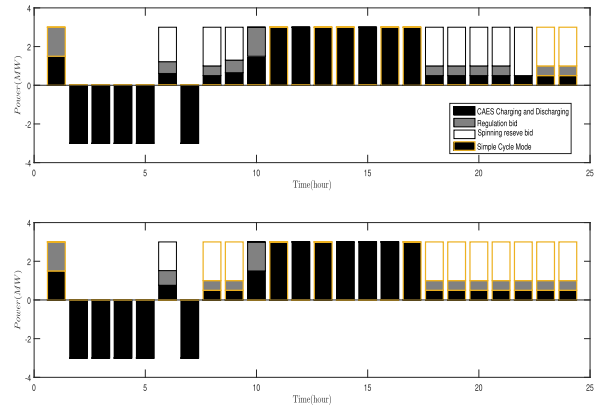


FIGURE 3. Compression and expansion of the CAES in coordinated mode in the first graph and in uncoordinated mode in the second graph.

TABLE 1. Profit comparison of wind plant and CAES coordinated and uncoordinated bids using DRO in energy (E) and ancillary services (AS) markets.

Methods	E and AS Markets	
Coordinated WP-CAES profit	Expected WC	5141.6
	Realization	5532.671
Uncoordinated WP profit	Expected WC	4033.4
	Realization	4239.549
Uncoordinated CAES profit	Expected WC	803.69
	Realization	1016.431

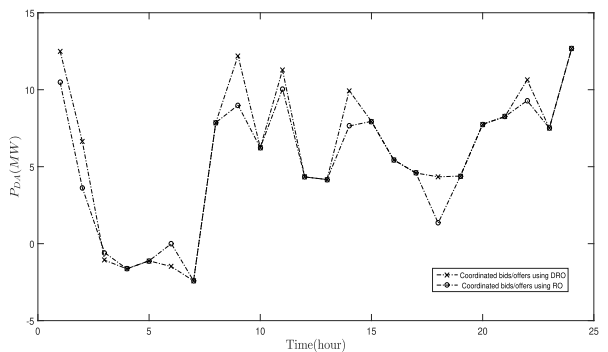


FIGURE 4. Case 1: coordinated bids/offers in day-ahead energy market.

using robust optimization. Case 1 considers the energy market alone, which has fewer uncertain parameters, and Case 2 utilizes the energy and ancillary service markets. This analysis will show a clear picture of how DRO outperforms robust optimization in dealing with uncertainty. A comparison of DRO and robust optimization of the day-ahead bids for Case 1 is illustrated in Fig. 4. Using RO results in more conservative bids compared to using DRO, as is shown in Hours 1, 2, 3, 6, 9, 11, 14, 18, and 22. This is because robust optimization generates bids based on worst-case scenarios without considering any statistical data.

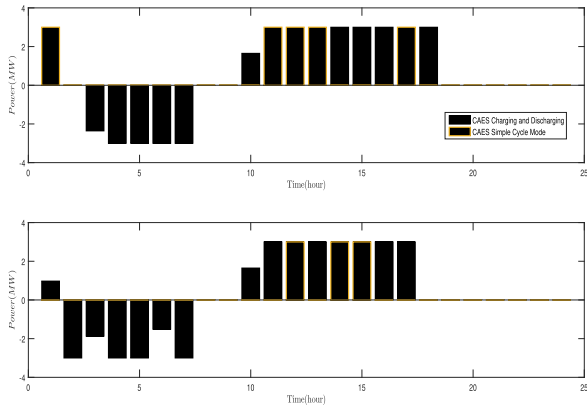


FIGURE 5. Case 1: CAES behavior in energy market using DRO in the first graph and using Robust Optimization in the second graph.

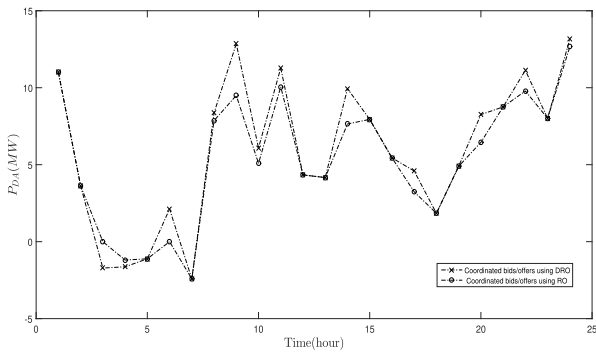


FIGURE 6. Case 2: coordinated bids/offers in day-ahead energy and ancillary service markets.

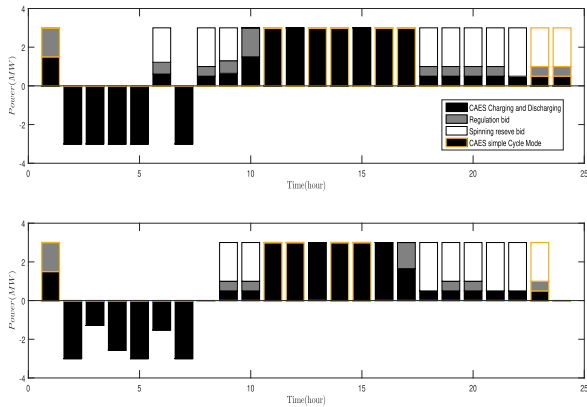


FIGURE 7. Case 2: CAESs behavior in energy and ancillary service markets using DRO in the first graph and using Robust Optimization in the second graph.

Similarly, Fig. 5 represents a slight difference in CAES behavior when participating in the energy market using DRO (a) and using robust optimization (b). At Hour 1, instead of discharging power at the rate of 1 MW/h using RO, when using DRO, the CAES stored energy, switching to simple cycle mode to provide more power. Fig. 6 and 7 represent in Case 2 coordinated system bids in energy and ancillary service markets. In this case, it is remarkable how the DRO’s ambiguity sets helped improve bid behavior in the day-ahead market as shown in Fig. 6, and participation in spinning reserve and regulation markets as presented in Fig. 7.

TABLE 2. Profit comparison of wind plant and CAES coordinated bids using DRO and Robust Optimization.

Methods		Case 1 (\$)	Case 2 (\$)
DRO	Expected WC	4524.9	5141.6
	Realization	4983.598	5532.671
RO	WC	4068.4	4472.7
	Realization	4725.489	5150.245

TABLE 3. Validation test comparison between DRO and robust optimization using Monte Carlo simulation.

Considered Market	DRO	95% CVaR	RO	95% CVaR
Case 1 (\$)	4578.72	3975.24	4312.35	4044.21
Case 2 (\$)	5187.22	4468.45	4824.34	4512.46

DRO and robust optimization bid scheduling are compared in Table (2). Expected worst-case profit and realized profit, which are calculated after the working day, are determined for the two markets using two-stage DRO. Similarly, worst-case profit and realized profit after the working day are calculated using robust optimization for each case. According to realized profits, robustness is guaranteed for both cases. However, incorporating statistical data yields better results for DRO than the more conservative ones of robust optimization. In additions, robust optimization bids according to worst-case wind power generation, resulting in higher deviations from actual wind power generation in the real time market.

D. VALIDATION TEST COMPARISON BETWEEN DRO AND ROBUST OPTIMIZATION BASED BIDDING STRATEGY USING MONTE CARLO SIMULATIONS WITH CONSIDERING THE CONDITIONAL VALUE AT RISK

Additionally, a Monte Carlo simulation was applied to the two cases and the profits of the combined wind-CAES system using DRO and RO were compared. Wind plant power output was assumed to follow a Gaussian distribution [39]. Similarly, Gaussian distributions were considered for market prices [40]. Accordingly, 1000 scenarios were generated for wind power generation, market prices, and reserve call signals to apply a validation test after bid submission. Profits were calculated for all the scenarios, and then the average profit was presented. The validation test was necessary to see the effectiveness of bid-based DRO compared to bid-based robust optimization in the scenarios generated from historical data. DRO and robust optimization were used to determine bids based on expected worst-case and worst-case wind power generation. As a result, in reality, there was extra power generated that could have been sold in the hour-ahead market at real-time prices, affecting the total profit.

A complete validation test comparison for the two cases is shown in Table (3). The total expected profits gained from

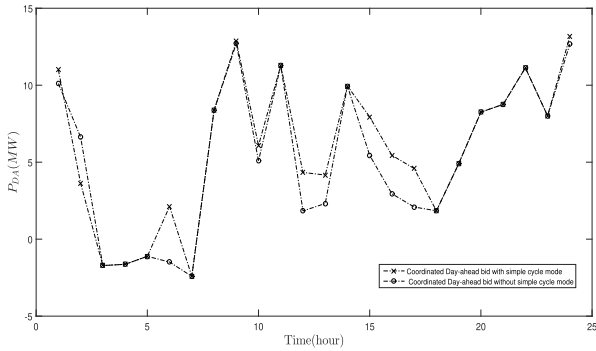


FIGURE 8. Coordinated Bids/Offers in day-ahead energy and ancillary services markets.

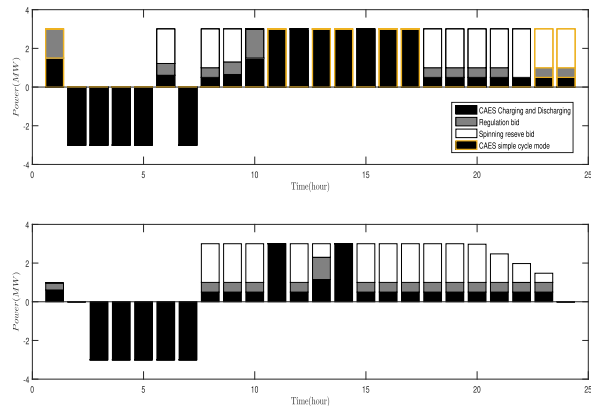


FIGURE 9. CAES behavior in energy and ancillary services markets With simple cycle operation mode in the first graph and Without simple cycle operation mode in the second graph.

participating in the energy market alone using DRO were higher than robust optimization by 5.8%. Considering the ancillary service market in the DRO and robust optimization problems added an extra \$608.5 and \$512 to the total profit, respectively. As a result, the gain using DRO would be higher by 7%. The third and fifth columns indicate the conditional value at risk (CVaR), which is the expected shortfall that measures and quantifies the tail risk associated with the 5% of all the scenarios generated from the bounded sets, without considering statistical measures. Robust optimization has a better CVaR because it produces the worst case scenario and its results are conservative against bounded sets.

E. COMPARISON OF COORDINATED BIDDING WITH AND WITHOUT THE SIMPLE CYCLE MODE OF THE CAES

Since the distinguishing difference of CAES compared to other energy storage systems is CAES’s ability to operate in simple cycle mode, this section illustrates the performance and profit of coordinated bidding with and without simple cycle mode. Fig. 8 represents day-ahead bids for the two cases. Incorporating simple cycle mode enhanced the bid curve at Hours 1, 2, 6, 10, 12, 13, 15, 16, 17, and 24. Also, as seen in the first graph of Fig. 9, at Hour 1, when the CAES did not have enough power, the CAES changed to simple cycle mode to exploit the benefit of high price, which was not the case in the second graph of Fig. 9. Furthermore, adding

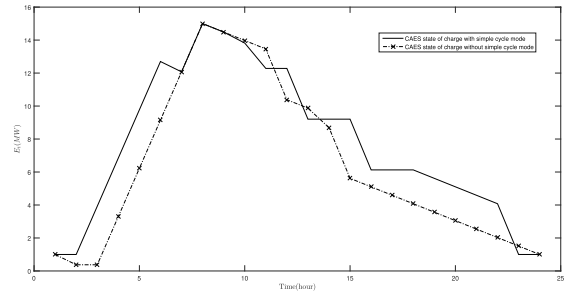


FIGURE 10. The state of charge (SOC) for the CAES with and without simple cycle operation mode during the operation time horizon.

TABLE 4. Profit comparison of wind plant and CAES coordinated bids using DRO with and without simple cycle operation mode.

Methods	Energy and Ancillary Service Markets (\$)	
With SC mode profit	Expected WC	5141.6
	Realization	5532.671
Without SC mode profit	Expected WC	4642.4
	Realization	5063.839

simple cycle operation mode to the CAES model increases the coordinated system’s options to seek more business opportunities. The dynamic behavior of the CAES (with and without simple cycle mode) is shown in Fig. 10. A CAES participating in an ancillary services market using simple cycle mode yields better performance and less risk since when an ISO sends capacity deployment signals to the wind-CAES system controller, it has more stored energy during each hour of the operation horizon.

Table (4) represents the expected worst-case profit and the realized profit after the operation day for coordinated system bids with and without simple cycle mode. A considerable amount of profit is added when the CAES operates in simple cycle mode. This remarkable gain spotlights the CAES system and makes it preferable to other energy storage systems.

F. THE EFFECT OF CAES CAPACITY SIZE ON THE WORST-CASE EXPECTED PROFIT

Different CAES capacity sizes were introduced to the case study, to evaluate the influence of CAES size on the hedging assigned to the wind plant used in this work. The worst-case expected profit was determined for each CAES size, starting from 5 to 60 MWh. Accordingly, modifications were carried out to the compression, expansion, and stat capacity with an equivalent rate of the CAES air reservoirs. The worst-case expected profits for each of the considered CAES capacities with and without simple cycle operation mode are shown in Figure (11). It is notable that as CAES capacity size increases in the two cases, a higher rate of profit accrues to the CAES using simple cycle operation mode. It is reasonable since increasing of the power rate of simple cycle mode will reduce its relative operation cost. Thus, determining the optimal size

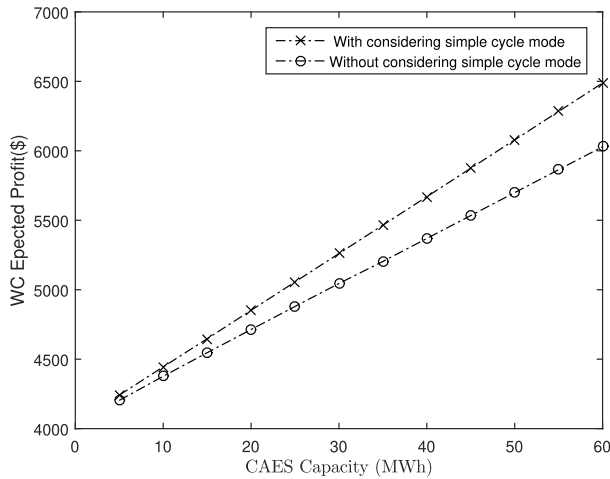


FIGURE 11. The influence of the CAES size on the profit.

of the CAES will result in greater efficiency and generate an optimal profit for the coordinated system.

VI. CONCLUSION

In this paper, coordinated bidding in a deregulated electricity market has been proposed by a combined system composed of wind plants and compressed air energy storage system. Simulation results showed that coordinating those two resources could improve profits while considering different constraints. CAES simple cycle mode was considered, where the CAES can work as a gas turbine when needed. This operating mode improved the profits more than ignoring it. Distributionally robust optimization was proposed to address uncertainties associated with wind plant power output, market prices, and regulation signals by incorporating ambiguity sets. Accordingly, an optimal bid scheduling strategy was obtained in energy and ancillary service markets. Comparison between robust optimization and DRO-based bidding strategies demonstrated that DRO gives rise to less conservative results and higher profit than robust optimization. This is due to the ability of DRO to incorporate statistical measures using historical data. Such an ability makes DRO preferable for the application of bidding capacity in the electricity market since ambiguity set can be generated using a wide range of ambiguous distribution information, allowing decision-makers to choose the uncertainty set based on the availability of historical data and their preference for solution robustness. However, robust optimization has a better-expected shortfall, yielding solutions that are deterministically robust to realizations of uncertain parameters in a certain set.

Future work could focus on improving the real-time bidding strategy of the CAES-wind plant with considering uncertainty associated with the hour ahead market. In order to enhance the utilization of wind power and reduce the overall cost of CAES, the optimal size of the CAES based on the proposed strategy could be investigated. One remaining issue for future work is determining the bidding strategy of the CAES-wind plant when it is a price maker.

APPENDIX

In classic robust optimization, the worst-case solution is determined based on the uncertainty sets. Therefore, the following generic min-max problem is solved using RO:

$$\min_{\mathbf{x} \in \mathbb{X}} \max_{\tilde{\mathbf{c}} \in \mathbb{C}} \{ \mathcal{L}(\mathbf{x}, \tilde{\mathbf{c}}) \} \quad (67)$$

$$\text{s.t. } g(\mathbf{x}, \tilde{\mathbf{c}}) \geq \mathbf{0} \quad (68)$$

\mathcal{L} and g are the objective and constraints, respectively. The uncertainties are molded using variable $\tilde{\mathbf{c}}$ which, belongs to the set \mathbb{C} where \mathbf{x} is a vector of decision variables which belong to set \mathbb{X} .

This paper adopted the work in [1] to extract uncertainty sets for \mathbb{C} . The scalar constant α is determined based on the budget of uncertainty Γ which is considered to be equal to one in our paper. Thus, the worst case optimal solution can be determined by solving the RO problem for the decision variables (DV) $\{P_t^w, P_t^d, P_t^{sc}, P_t^{ch}, P_t^{d, sr}, P_t^{sc, sr}, P_t^{d, reg}, P_t^{sc, reg}\}$ and uncertain parameters (UP) $\{\gamma^e, \gamma^{sr}, \gamma^{reg}, \gamma^{reg, m}, \gamma^{rt}\}$, as follows:

$$\begin{aligned} \min_{DV} \max_{UP} \sum_{t \in T} & -[\gamma_t^e \cdot P_t^{DA} + \gamma_t^{sr} \cdot (P_t^{d, sr} + P_t^{sc, sr}) + \gamma_t^{reg} \\ & \cdot (P_t^{d, reg} + P_t^{sc, reg}) + \gamma_t^{rt} \cdot \alpha^{sr} \cdot (P_t^{d, sr} + P_t^{sc, sr}) \\ & + \gamma_t^{reg, m} R_{mil} (P_t^{d, reg} + P_t^{sc, reg}) - OC] \end{aligned} \quad (69)$$

The constraints of the wind-CAES system are defined previously in the objective and constraints section; see (2) to (16). The uncertainty sets of market prices and wind plant generation are defined as follows:

$$\mathcal{P}^\kappa = [(1 - \alpha^\kappa) \boldsymbol{\gamma}^\kappa, (1 + \alpha^\kappa) \boldsymbol{\gamma}^\kappa], \quad \kappa = (e, sr, reg, rt) \quad (70)$$

$$\mathcal{W} = [(1 - \alpha^s) \mathbf{P}^s, (1 + \alpha^s) \mathbf{P}^s] \quad (71)$$

After moving the objective function to the constraints by an epigraph reformulation and taking the dual of the inner maximization subproblem, the problem is converted into a tractable MILP formulation. Then, the problem can be solved in MATLAB using the intlinprog solver and YALMIP toolbox.

REFERENCES

- [1] A. A. Thatte and D. E. Viassolo, "Robust bidding strategy for wind power plants and energy storage in electricity markets," in *Proc. IEEE Power Energy Soc. Gen. Meeting*, Jul. 2012, pp. 1–7.
- [2] L. W. Chong, Y. W. Wong, R. K. Rajkumar, R. K. Rajkumar, and D. Isa, "Hybrid energy storage systems and control strategies for stand-alone renewable energy power systems," *Renew. Sustain. Energy Rev.*, vol. 66, pp. 174–189, Dec. 2016.
- [3] H. Ding, Z. Hu, and Y. Song, "Rolling optimization of wind farm and energy storage system in electricity markets," *IEEE Trans. Power Syst.*, vol. 30, no. 5, pp. 2676–2684, Sep. 2015.
- [4] R. Hemmati and N. Azizi, "Advanced control strategy on battery storage system for energy management and bidirectional power control in electrical networks," *Energy*, vol. 138, pp. 520–528, Nov. 2017. [Online]. Available: <http://www.sciencedirect.com/science/article/pii/S0360544217312471>
- [5] S. Ghavidel, M. J. Ghadi, A. Azizivahed, J. Aghaei, L. Li, and J. Zhang, "Risk-constrained bidding strategy for a joint operation of wind power and CAES aggregators," *IEEE Trans. Sustain. Energy*, vol. 11, no. 1, pp. 457–466, Jan. 2020.

- [6] H. Akhavan-Hejazi and H. Mohsenian-Rad, "Optimal operation of independent storage systems in energy and reserve markets with high wind penetration," *IEEE Trans. Smart Grid*, vol. 5, no. 2, pp. 1088–1097, Mar. 2014.
- [7] X. He, R. Lecomte, A. Nekrassov, E. Delarue, and E. Mercier, "Compressed air energy storage multi-stream value assessment on the French energy market," in *Proc. IEEE Trondheim PowerTech*, Jun. 2011, pp. 1–6.
- [8] S. Kahrobaee and S. Asgarpour, "Optimum planning and operation of compressed air energy storage with wind energy integration," in *Proc. North American Power Symp. (NAPS)*, Sep. 2013, pp. 1–6.
- [9] B. Mauch, P. M. S. Carvalho, and J. Apt, "Can a wind farm with CAES survive in the day-ahead market?" *Energy Policy*, vol. 48, pp. 584–593, Sep. 2012. [Online]. Available: <http://www.sciencedirect.com/science/article/pii/S0301421512004740>
- [10] R. Khatami, K. Oikonomou, and M. Parvania, "Look-ahead optimal participation of compressed air energy storage in day-ahead and real-time markets," *IEEE Trans. Sustain. Energy*, vol. 11, no. 2, pp. 682–692, Apr. 2020.
- [11] H. Zareipour, A. Janjani, H. Leung, A. Motamedi, and A. Schellenberg, "Classification of future electricity market prices," *IEEE Trans. Power Syst.*, vol. 26, no. 1, pp. 165–173, Feb. 2011.
- [12] A. Attarha, N. Amjadi, S. Dehghan, and B. Vatani, "Adaptive robust self-scheduling for a wind producer with compressed air energy storage," *IEEE Trans. Sustain. Energy*, vol. 9, no. 4, pp. 1659–1671, Oct. 2018.
- [13] E. Akbari, R.-A. Hooshmand, M. Gholipour, and M. Parastegari, "Stochastic programming-based optimal bidding of compressed air energy storage with wind and thermal generation units in energy and reserve markets," *Energy*, vol. 171, pp. 535–546, Mar. 2019. [Online]. Available: <http://www.sciencedirect.com/science/article/pii/S0360544219300167>
- [14] Z. Guo, W. Wei, L. Chen, Z. Wang, and S. Mei, "Operation of distribution network considering compressed air energy storage unit and its reactive power support capability," *IEEE Trans. Smart Grid*, vol. 11, no. 4, pp. 2954–2965, Jul. 2020.
- [15] J. Bai, W. Wei, L. Chen, and S. Mei, "Modeling and dispatch of advanced adiabatic compressed air energy storage under wide operating range in distribution systems with renewable generation," *Energy*, vol. 206, Sep. 2020, Art. no. 118051. [Online]. Available: <https://www.sciencedirect.com/science/article/pii/S0360544220311580>
- [16] H. Khaloie, A. Abdollahi, M. Shafie-Khah, P. Siano, S. Nojavan, A. Anvari-Moghaddam, and J. P. S. Catalão, "Co-optimized bidding strategy of an integrated wind-thermal-photovoltaic system in deregulated electricity market under uncertainties," *J. Cleaner Prod.*, vol. 242, Jan. 2020, Art. no. 118434. [Online]. Available: <http://www.sciencedirect.com/science/article/pii/S0959652619333049>
- [17] H. Khaloie, A. Abdollahi, M. Shafie-khah, A. Anvari-Moghaddam, S. Nojavan, P. Siano, and J. P. S. Catalão, "Coordinated wind-thermal-energy storage offering strategy in energy and spinning reserve markets using a multi-stage model," *Appl. Energy*, vol. 259, Feb. 2020, Art. no. 114168. [Online]. Available: <http://www.sciencedirect.com/science/article/pii/S0306261919318550>
- [18] H. Mohsenian-Rad, "Coordinated price-maker operation of large energy storage units in nodal energy markets," *IEEE Trans. Power Syst.*, vol. 31, no. 1, pp. 786–797, Jan. 2016.
- [19] A. T. Al-Awami, N. A. Amleh, and A. M. Muqbel, "Optimal demand response bidding and pricing mechanism with fuzzy optimization: Application for a virtual power plant," *IEEE Trans. Ind. Appl.*, vol. 53, no. 5, pp. 5051–5061, Sep. 2017.
- [20] S. Nojavan, A. Najafi-Ghalelou, M. Majidi, and K. Zare, "Optimal bidding and offering strategies of merchant compressed air energy storage in deregulated electricity market using robust optimization approach," *Energy*, vol. 142, pp. 250–257, Jan. 2018. [Online]. Available: <http://www.sciencedirect.com/science/article/pii/S0360544217316973>
- [21] A. A. Thatte, L. Xie, D. E. Viassolo, and S. Singh, "Risk measure based robust bidding strategy for arbitrage using a wind farm and energy storage," *IEEE Trans. Smart Grid*, vol. 4, no. 4, pp. 2191–2199, Dec. 2013.
- [22] T. Zhao, X. Pan, S. Yao, C. Ju, and L. Li, "Strategic bidding of hybrid AC/DC microgrid embedded energy hubs: A two-stage chance constrained stochastic programming approach," *IEEE Trans. Sustain. Energy*, vol. 11, no. 1, pp. 116–125, Jan. 2020.
- [23] Q. Bian, H. Xin, Z. Wang, D. Gan, and K. P. Wong, "Distributionally robust solution to the reserve scheduling problem with partial information of wind power," *IEEE Trans. Power Syst.*, vol. 30, no. 5, pp. 2822–2823, Sep. 2015.
- [24] C. Duan, L. Jiang, W. Fang, J. Liu, and S. Liu, "Data-driven distributionally robust energy-reserve-storage dispatch," *IEEE Trans. Ind. Informat.*, vol. 14, no. 7, pp. 2826–2836, Jul. 2018.
- [25] W. Wei, F. Liu, and S. Mei, "Distributionally robust co-optimization of energy and reserve dispatch," *IEEE Trans. Sustain. Energy*, vol. 7, no. 1, pp. 289–300, Jan. 2016.
- [26] P. Xiong, P. Jirutitijaroen, and C. Singh, "A distributionally robust optimization model for unit commitment considering uncertain wind power generation," *IEEE Trans. Power Syst.*, vol. 32, no. 1, pp. 39–49, Jan. 2017.
- [27] F. Alismail, P. Xiong, and C. Singh, "Optimal wind farm allocation in multi-area power systems using distributionally robust optimization approach," *IEEE Trans. Power Syst.*, vol. 33, no. 1, pp. 536–544, Jan. 2018.
- [28] M. Kazemi, H. Zareipour, N. Amjadi, W. D. Rosehart, and M. Ehsan, "Operation scheduling of battery storage systems in joint energy and ancillary services markets," *IEEE Trans. Sustain. Energy*, vol. 8, no. 4, pp. 1726–1735, Oct. 2017.
- [29] *Market Participants User's Guide: Guide 01, Version 11.3*, NYISO Stakeholder Services, Rensselaer, NY, USA, 2021. Accessed: Aug. 25, 2021. [Online]. Available: <https://www.nyiso.com/documents/20142/3625950/mpug.pdf>
- [30] J. Garcia-Gonzalez, R. M. R. de la Muela, L. M. Santos, and A. M. Gonzalez, "Stochastic joint optimization of wind generation and pumped-storage units in an electricity market," *IEEE Trans. Power Syst.*, vol. 23, no. 2, pp. 460–468, May 2008.
- [31] C. Shang and F. You, "Distributionally robust optimization for planning and scheduling under uncertainty," *Comput. Chem. Eng.*, vol. 110, pp. 53–68, Feb. 2018. [Online]. Available: <http://www.sciencedirect.com/science/article/pii/S009813541730426X>
- [32] D. Bertsimas, V. Gupta, and N. Kallus, "Data-driven robust optimization," 2014, *arXiv:1401.0212*.
- [33] D. Bertsimas, V. Gupta, and N. Kallus, "Data-driven robust optimization," *Math. Program.*, vol. 167, no. 2, pp. 235–292, Feb. 2018, doi: [10.1007/s10107-017-1125-8](https://doi.org/10.1007/s10107-017-1125-8).
- [34] X. Chen, M. Sim, P. Sun, and J. Zhang, "A linear decision-based approximation approach to stochastic programming," *Oper. Res.*, vol. 56, no. 2, pp. 344–357, 2008.
- [35] A. Ben-Tal, A. Goryashko, E. Guslitzer, and A. Nemirovski, "Adjustable robust solutions of uncertain linear programs," *Math. Program.*, vol. 99, no. 2, pp. 351–376, 2004, doi: [10.1007/s10107-003-0454-y](https://doi.org/10.1007/s10107-003-0454-y).
- [36] X. Chen and Y. Zhang, "Uncertain linear programs: Extended affinely adjustable robust counterparts," *Oper. Res.*, vol. 57, no. 6, pp. 1469–1482, Nov. 2009.
- [37] *Market and Operation Data-Pricing Database*, New York Independ. Syst. Operator, Rensselaer, NY, USA, 2016.
- [38] *Wind Toolkit Offshore Summary Dataset*, NRE Laboratory, Medan, IN, USA, 2017.
- [39] X.-Y. Ma, Y.-Z. Sun, and H.-L. Fang, "Scenario generation of wind power based on statistical uncertainty and variability," *IEEE Trans. Sustain. Energy*, vol. 4, no. 4, pp. 894–904, Oct. 2013.
- [40] M. E. Hajiabadi and H. R. Mashhadi, "Analysis of the probability distribution of LMP by central limit theorem," *IEEE Trans. Power Syst.*, vol. 28, no. 3, pp. 2862–2871, Aug. 2013.

• • •